Science Advances
AAAS

advances.sciencemag.org/cgi/content/full/6/25/eaaz3621/DC1

Supplementary Materials for

Microneedle-mediated gene delivery for the treatment of ischemic myocardial disease

Hongpeng Shi, Tong Xue, Yang Yang, Chenyu Jiang, Shixing Huang, Qi Yang, Dong Lei, Zhengwei You, Tuo Jin, Fei Wu*, Qiang Zhao*, Xiaofeng Ye*

*Corresponding author. Email: xiaofengye@hotmail.com (X.Y.); zq11607@rjh.com.cn (Q.Z.); feiwu@sjtu.edu.cn (F.W.)

Published 17 June 2020, *Sci. Adv.* **6**, eaaz3621 (2020)
DOI: 10.1126/sciadv.aaz3621

The PDF file includes:

Other Supplementary Material for this manuscript includes the following:

(available at advances.sciencemag.org/cgi/content/full/6/25/eaaz3621/DC1)

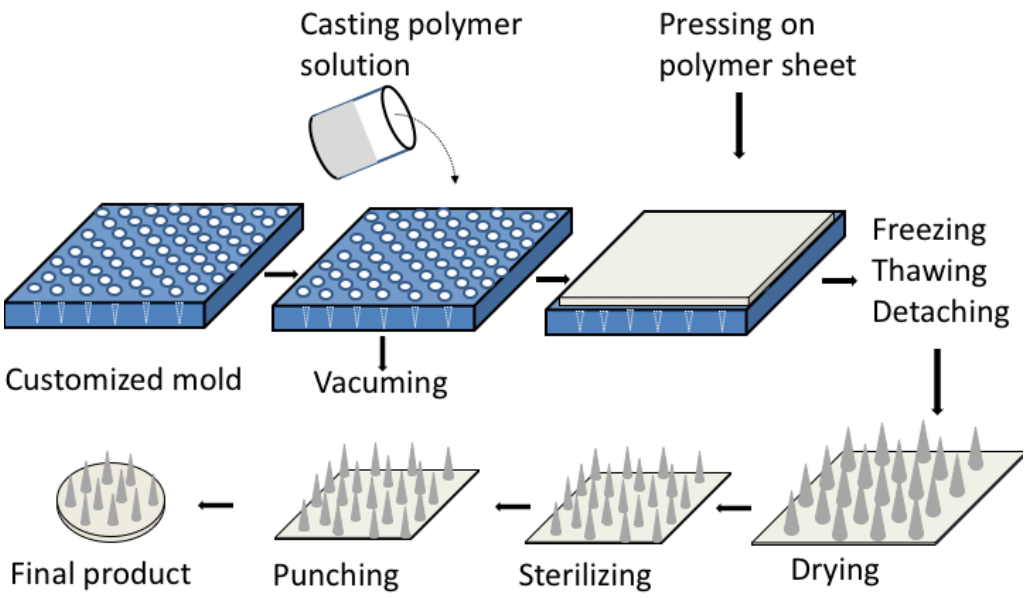

Fig. S1. Schematic of the experimental procedures performed to illustrate the fabrication process of the MNs.

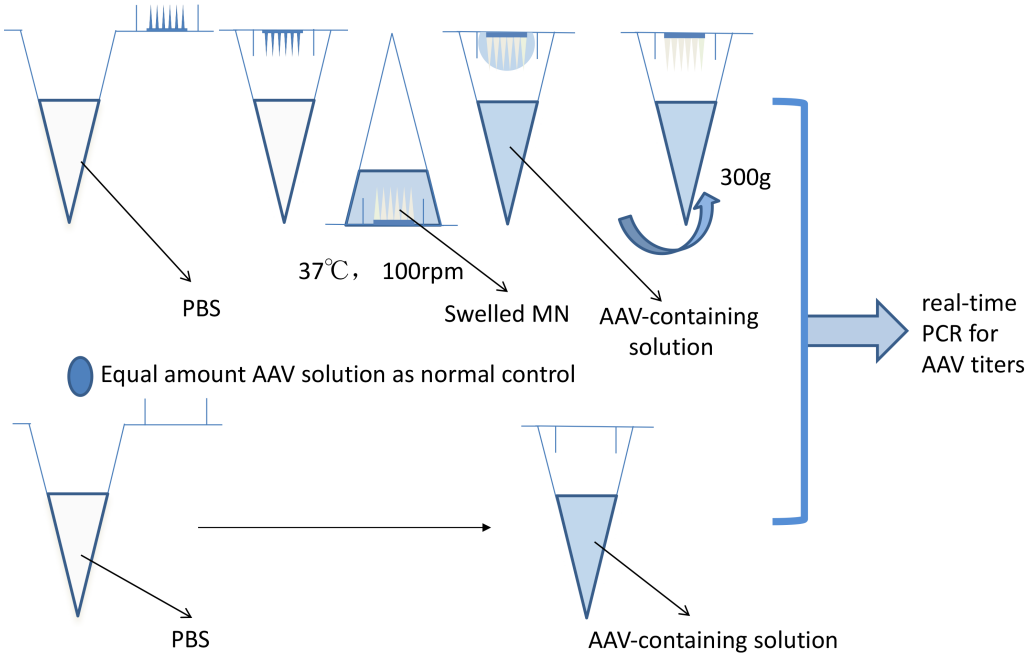

Fig. S2. Schematic of the experimental procedures performed to collect the released AAV fluid.

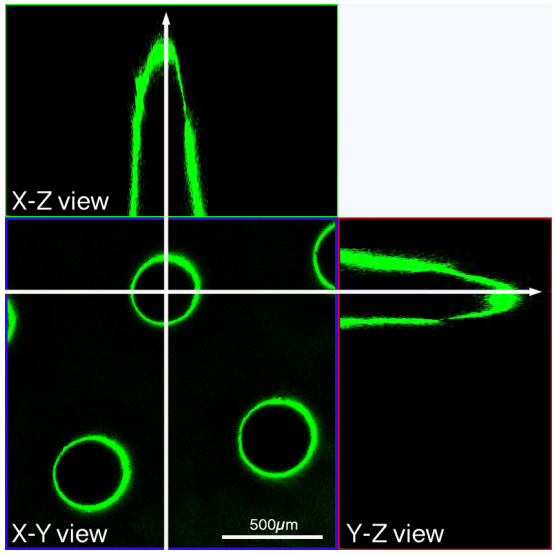

Fig. S3. The ortho view generated from a confocal laser scanning micrograph of z-stack images visualizes the MN tip as transverse section (x–y) and lateral sections (x–z, y–z) views.

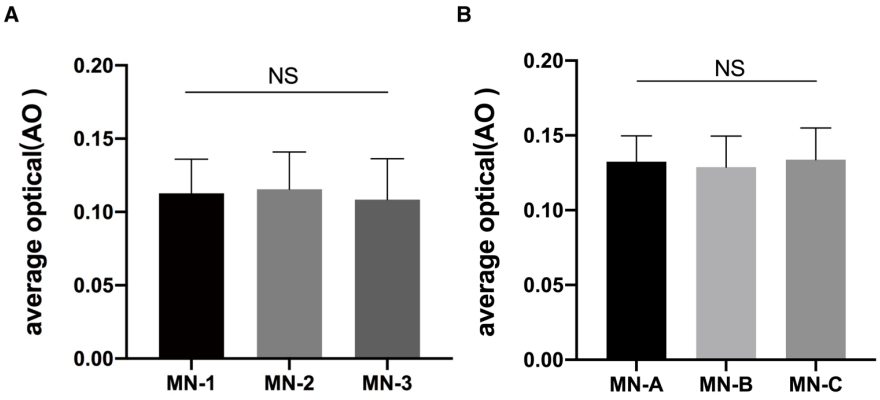

Fig. S4. Uniformity of MN-AAV. (A) Comparison of fluorescence intensity among three MN patches. (B) Comparison of fluorescence intensity among three rat hearts that received MN-FITC-AAV (15 puncture points were analyzed in each fluorescent image). NS, not significant.

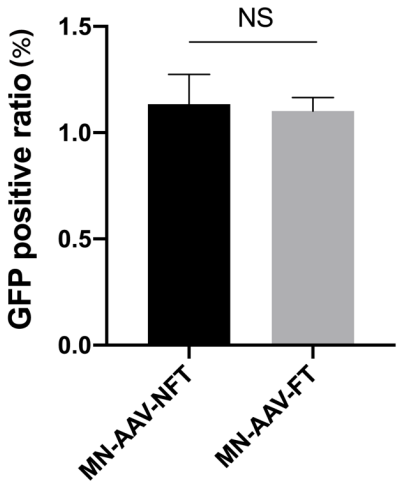

Fig. S5. Tolerance of MN-AAV subjected or not subjected to the freeze-thaw process. MN-AAV-NFT represents virus-containing MNs not subjected to the freeze-thaw process. MN-AAV-FT represents virus-containing MNs subjected to the freeze-thaw process. n=5 patches in each group. NS, not significant.

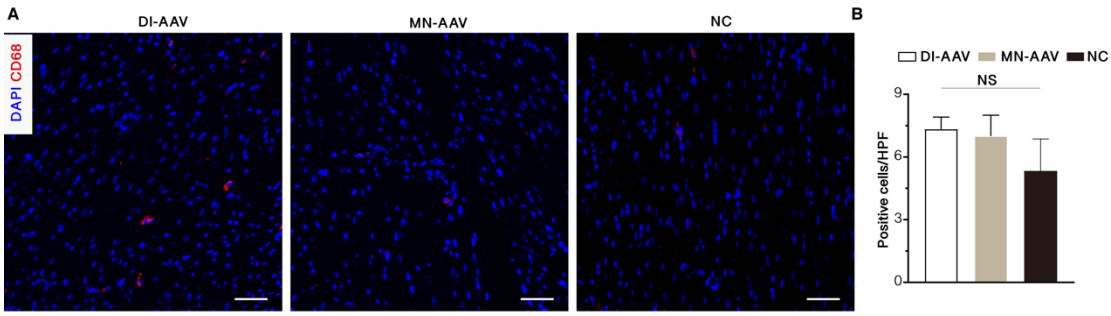

Fig. S6. Inflammatory response in the MN-AAV group compared with the DI-AAV and NC groups. Histogram showing the numbers of positive cells in the three groups. n = 3 hearts for each group. Scale bar: 50 μm. NS, not significant.

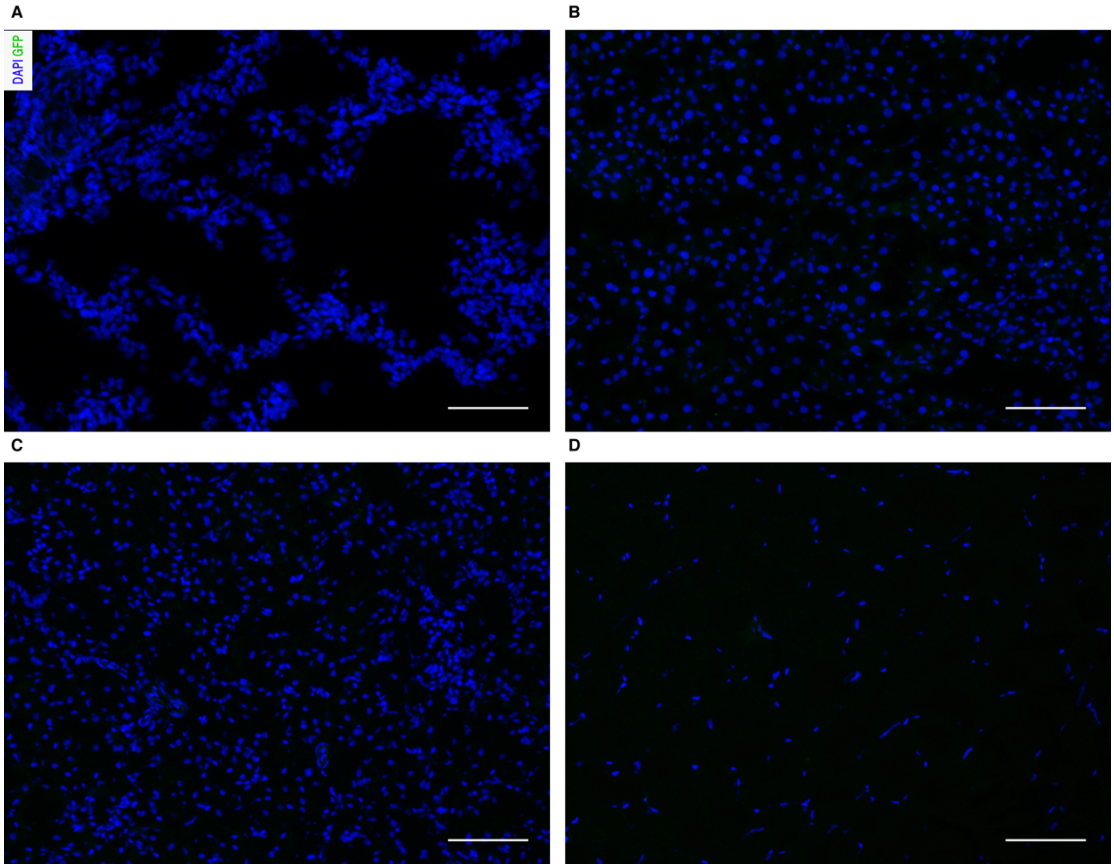

Fig. S7. Determination of vector dissemination to off-target organs. (A) Lungs. (B) Liver. (C) Kidneys. (D) Skeletal muscles. Lung, liver, kidney and skeletal muscle tissues were harvested 4 weeks following MN-AAV-GFP application. No GFP expression was found in the above organs and tissues. n = 3 rats for each organ. Scale bar: 100 μm.

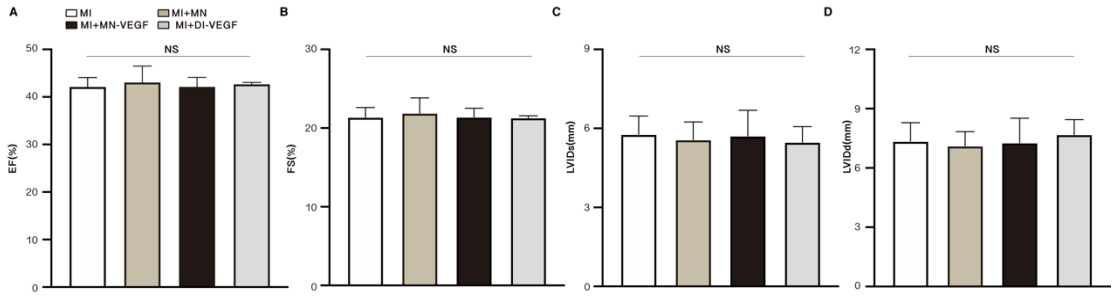

Fig. S8. Heart performance parameters measured at baseline did not significantly differ among the four groups. (A) EF. (B) FS. (C) LVIDs. (D) LVIDd. NS, not significant.

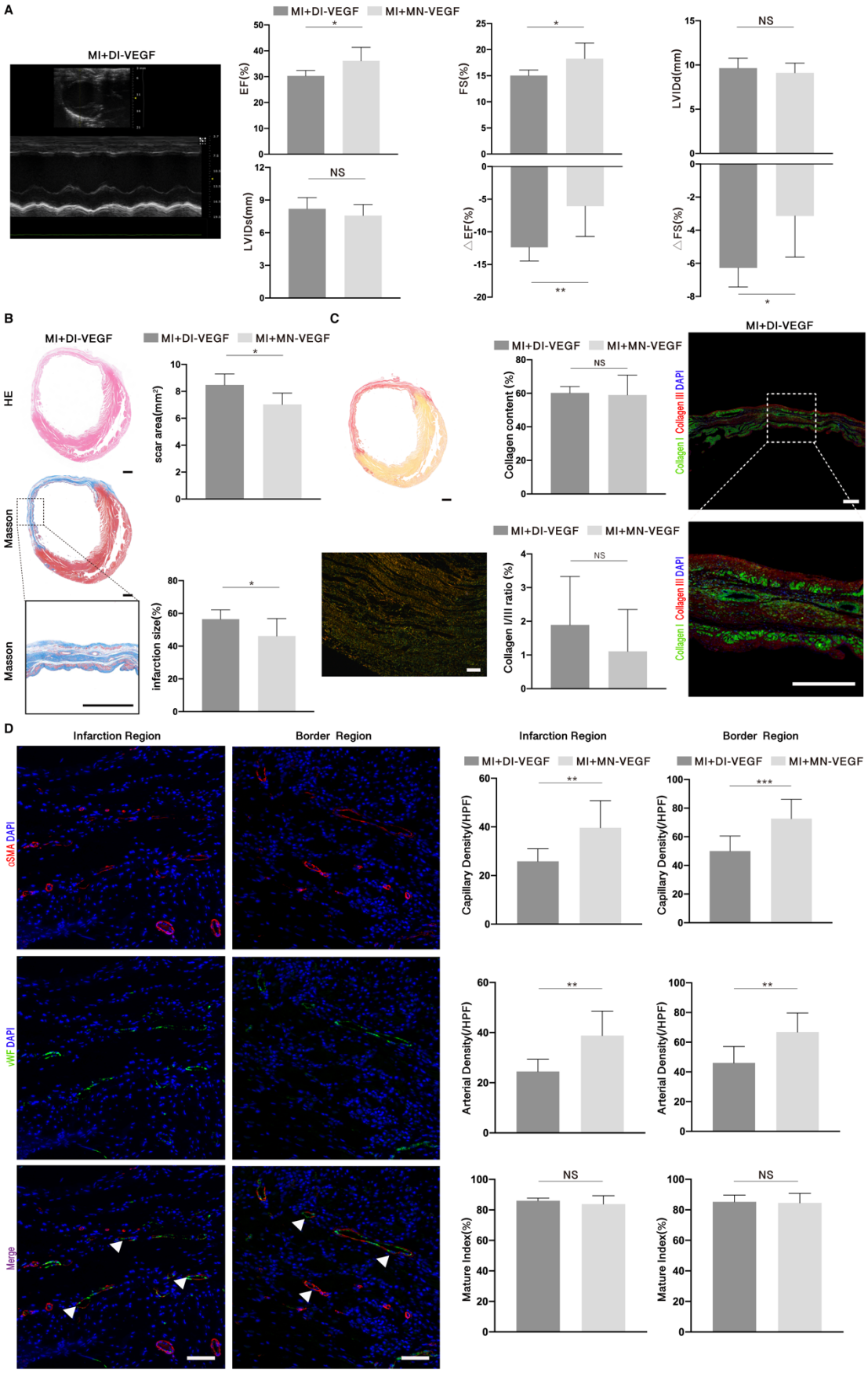

Fig. S9. Parameters of the MI+DI-VEGF group. (A) Representative echocardiographic images and heart performance of the MI+DI-VEGF group compared with the MI+MN-VEGF group (EF, FS, LVIDs, LVIDd,

ΔEF and ΔFS). (B) Representative Masson's trichrome-stained myocardial sections and quantitative analyses of the scar areas and infarct sizes compared with those in the MI+MN-VEGF group. Scale bar: 1 mm. (C) Identification of collagens via picrosirius red staining (Scale bar: 1 mm), polarized light microscopy (Scale bar: 100 μm) and fluorescence staining (type I collagen was stained green, and type III collagen was stained red; Scale bar: 500 μm). The histograms show comparisons of the collagen content and the type I/type III collagen ratios between the MI+DI-VEGF and MI+MN-VEGF groups. (D) Representative immunofluorescent images of vWF (green) and αSMA (red) in the tissues of the infarction and border regions (n = 3 animals per group; Scale bar: 50 μm). The histograms show the values and comparisons of capillary density, arterial density and the mature index between the MI+DI-VEGF and MI+MN-VEGF groups. *p<0.05, **p<0.01 and ***p<0.001. NS, not significant.

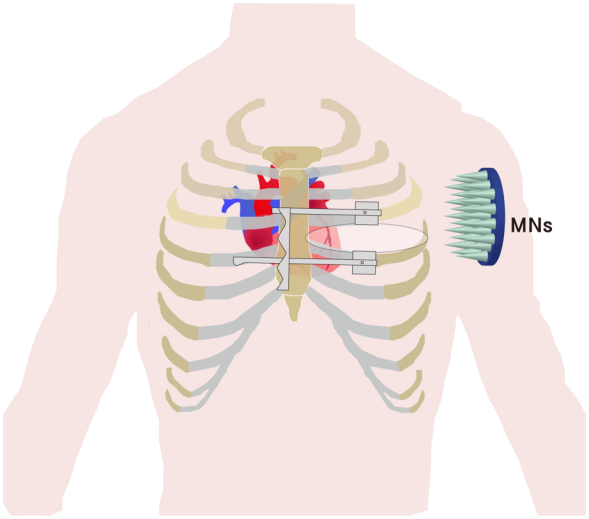

Fig. S10. Schematic diagram of our vision for translation of the MNs into the clinic. The patient is receiving MNs via a small thoracic incision.

Movie S1. Application of a customized MN apparatus without MN loading.
Movie S2. Rat heart following MN application.
Movie S3. Application of methylene blue-loaded MNs via a customized adapter.
Movie S4. Rat heart following the application of methylene blue-loaded MNs.

Table S1. Antibodies used in the current study.

Antibody	Source; Cat. No.	Application	Notes
Anti-human VEGF165	R&D; AF-293-NA	WB[a]	Primary Ab
Anti-VEGF receptor 2	CST; #12634	WB	Primary Ab
Anti-PI3 kinase	CST; #4249	WB	Primary Ab
Anti-Akt	CST; #4691	WB	Primary Ab
Anti-p-Akt	CST; #13038	WB	Primary Ab
Anti-Caspase9	Abcam; ab2013	WB	Primary Ab
Anti-GAPDH	Proteintech; 60004-1-Ig	WB	Primary Ab
Anti-luciferase	Abcam; ab181640	WB	Primary Ab
Anti-von Willebrand factor	Abcam; ab6994	IF[b]	Primary Ab
Anti-αSMA	Abcam; ab5694	IF	Primary Ab
Anti-Collagen I	Abcam; ab34710	IF	Primary Ab
Anti-Collagen III	Abcam; ab7778	IF	Primary Ab
Anti-CD68	Abcam; ab125212	IF	Primary Ab
Anti-Anti-cTnT	Abcam; ab8295	IF	Primary Ab
Goat anti-rabbit Alexa Fluor® 488	Invitrogen; A-11008	IF	Secondary Ab
Goat anti-mouse Alexa Fluor® 594	Invitrogen; A-11032	IF	Secondary Ab
Goat anti-rabbit Alexa Fluor® 594	Invitrogen; A-11012	IF	Secondary Ab

a, Western blot; b, immunofluorescence